A New Image Watermarking Algorithm Using the Contourlet Transform and the Harris Detector

Dandan Zhu[1,2(✉)] and Lizhi Lv[3]

[1] College of Information Science and Engineering, Northeastern University, Shenyang 110819, China
zhudan0526@163.com
[2] Department of Computer Science, Tonghua Normal University, Tonghua 134000, China
[3] College of Computer Science and Technology, Taiyuan University of Technology, Taiyuan 030024, China

Abstract. In this paper, we propose a new feature-based image watermarking scheme based on multiscale theory and the Contourlet transform (CT). We use the multiscale Harris detector to extract stable feature points from the host image. Next, according to feature scale theory, we determine the local feature regions (LFR) and scale the regions to a standard size. We then embed the digital watermark into the Contourlet low frequency area calculated using the pseudo-Zernike moment. The results of our experiments demonstrate that the algorithm results in an invisible watermark and is robust against conventional signal processing (median filtering, sharpening, noise adding, and JPEG compression), geometric attacks (rotation, translation, scaling, row or column removal, shearing, local geometric distortion) and combined attacks.

Keywords: Image watermarking · Geometric attacks · Contourlet transform · Pseudo-Zernike moments · Low sub-band1

1 Introduction

Digital watermarking is widely used in Internet multimedia intellectual property protection [1-2]. Great progress has been achieved in the image transform domain by applying the discrete cosine transform (DCT)[3-4] and discrete wavelet transform (DWT)[5-6] in digital watermarking algorithms. However, these theories do not adequately represent the anisotropy of signals. The Ridgelet [7], Curvelet [8], and Concourlet [9] transforms better address the anisotropy of signals and can effectively resist Random bending attack (RBA), Geometric attacks (i.e., Rotation, Scale and Translation, RST), and Shearing. Many methods have been proposed to evade geometric attacks. These methods can be roughly divided into three categories: (1) invariant transforms [12-13], which are robust against global geometrical distortion but not against shearing; (2) feature-based synchronization [14-15], whose watermarking capacity is very limited; and (3) template insertion [16], which cannot withstand any malicious attacks.

H. Zha et al. (Eds.): CCCV 2015, Part II, CCIS 547, pp. 439–447, 2015.
DOI: 10.1007/978-3-662-48570-5_42

To address the above problems, we present a new digital watermarking scheme, which includes two main features. First, an analysis of Contourlet transform characteristics indicates that the proposed scheme can adaptively embed a watermark into low frequency sub-bands with many textures. Second, we review feature-based synchronization methods and propose a novel watermark synchronization strategy. In experiments, we compare the performance of the proposed algorithm with other algorithms by applying various attacks. The results demonstrate the superior robustness of the proposed watermarking algorithm.

2 Contourlet Transform

The Contourlet transform is a geometrical transform that uses multiresolution analysis and multi-direction analysis to effectively show the contour and texture of an image. The basis functions of the Contourlet transform provide different scales and thus extend support for the aspect ratio, assuming that linear and face discontinuities are preferred. Compared with the wavelet transform, the Contourlet transform offers more and richer basis functions. It can use fewer coefficients to represent smooth edges and combine the discontinuity points with the same directionality into a discontinuity line or face. The main characteristics of the Contourlet are compared with those of DWT in Figure 1.

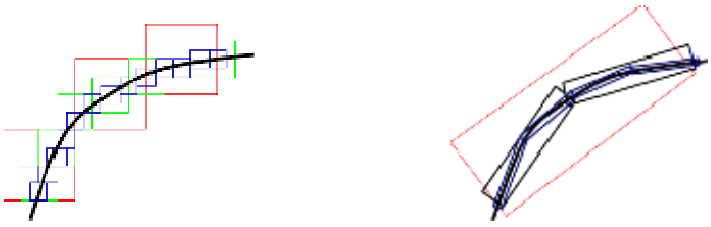

(a) DWT (b) Contourlet

Fig. 1. Comparison of basis functions

3 Scale-Adaptive Harris Detector

The Harris detector is based on the second moment matrix [17] which is an image descriptor reflecting the distribution of the local gradient directions of the image. The scale-adaptive second moment matrix is defined as:

$$M(x, y, \delta_I, \delta_D) = \delta_D^2 \cdot G(\delta_I) * \begin{bmatrix} L_x^2(x, y, \delta_D) & L_x L_y(x, y, \delta_D) \\ L_x L_y(x, y, \delta_D) & L_y^2(x, y, \delta_D) \end{bmatrix} \tag{1}$$

δ_I denotes the integration scale, δ_D denotes the differentiation scale, and L_a denotes the partial derivative in the a direction. The uniform Gaussian scale space representation L is defined as:

$$L(x, y, \delta_D) = G(x, y, \delta_D) * f \tag{2}$$

Here, G denotes the Gaussian function with zero mean and δ_D is the standard deviation. f denotes the image and $*$ indicates linear convolution.

Given δ_I and δ_D, the second moment matrix $M(x, y, \delta_I, \delta_D)$ can be used to compute the scale-adaptive Harris corner strength (SHCS) detector:

$$\begin{aligned} &R(x, y, \delta_I, \delta_D) \\ &\quad = Det\left(M\left(x, y, \delta_I, \delta_D\right)\right) - k \cdot Tr^2\left(M\left(x, y, \delta_I, \delta_D\right)\right) \end{aligned} \tag{3}$$

Here $Det(\bullet)$ denotes the determinant of the matrix and $Tr(\bullet)$ is the trace. At each scale-space level, the feature points are extracted according to the following rules:

$$\begin{aligned} &R(x, y, \delta_I, \delta_D) > R(\hat{x}, \hat{y}, \delta_I, \delta_D) \qquad \forall (\hat{x}, \hat{y}) \in A \\ &R(x, y, \delta_I, \delta_D) \geq t_u \end{aligned} \tag{4}$$

Here, A is the neighborhood of pixel (x, y) and t_u is the threshold.

Automatic Scale Selection and Scale-Invariant Feature Points

We use the Laplacian-of-Gaussians (LOG) operator to determine the characteristic scale. The LOG is defined as:

$$LOG(x, y, \delta_I) = \delta_I^2 \left| \frac{\partial^2 G(x, y, \delta_I)}{\partial x^2} + \frac{\partial^2 G(x, y, \delta_I)}{\partial y^2} \right| \tag{5}$$

$$LOG = \frac{1}{10}\left(6 \cdot LOG_Y + 2 \cdot LOG_{Cb} + 2 \cdot LOG_{Cr}\right) \tag{6}$$

The steps to extract feature points using the Harris-Laplace detector are as follows:

(i) A scale-space representation is built with the Harris function for the preselected scales $\delta_n = 1.4\xi^n$, where ξ denotes the scale factor between continuous levels. At each representation level, the SHCS is computed with $\delta_I = \delta_n$ and $\delta_D = s\delta_n$ (s is a constant). After that, the candidate points that are maximal in the 8-neighborhood with SHCS greater than $t_u = 1000$ are extracted.

(ii) An iterative algorithm is applied to compute each candidate point's scale and location. The scales of feature points are selected by the extrema over the LOG scale.

For an initial point p having scale δ_I, the iteration scheme can be described as the following:

1) For a point p_k, search its local extremum over the LOG scale, otherwise reject it. Limit the investigated scope of the scale to $\delta_I^{(k+1)} = t \cdot \delta_I^{(k)}$ with $t \in [0.7, \cdots, 1.4]$.

2) Search the spatial point p_{k+1} of a maximum of the SHCS nearest to p_k for $\delta_I^{(k+1)}$.

3) Return to Step 1 until $\delta_I^{(k+1)} = \delta_I^{(k)}$ or $p_{k+1} = p_k$.

Local Characteristic Regions

We consider the problem of geometric synchronization in our choice of LCR construction method. We select a circular area that is independent of image rotation and determine its size by the characteristic scale. Define the radius $\Re$ of the LCRs as:

$$\Re = \tau \cdot \lceil \delta \rceil \tag{7}$$

Here δ denotes the characteristic scale and τ denotes a positive integer to adjust the size of the LCRs. The robustness of the CBIR system increases for a small LCR while the capacity decreases. Thus, there is a tradeoff between these two factors. The theoretical range of $\Re$ is:

$$round(\delta) \le \Re \le \frac{\min(M, N)}{2} \tag{8}$$

We reserve the LCR with the highest SHCS and discard the others as the higher SHCS indicates a more robust feature point.

4 Watermark Embedding Algorithm

Watermark embedding can be regarded as an additive process of a strong background signal (the original image) and a weak signal (the watermark). The watermark is embedded into the significant features. The embedding scheme can be decomposed into the following seven steps:

1) Generate a random sequence $W = \{w_i, i = 1, \cdots, L\}$ using the secret key K_1, where the sequence values are $w_i \in \{0,1\}$ and L denotes the size of the sequence.

2) Apply the Harris-Laplace detector to the host image to obtain a feature point set $P = \{p_i, i = 1, \cdots, n\}$. Use these points for the reference centers of the local feature regions.

3) Use our proposed method to construct the local feature regions $O = \{o_k, k = 1, \cdots, m\}$.

4) Perform a zero-padding operation on each $o_k \in O$. Apply the normalization procedure to each block of size $2R_K \times 2R_K$ (R_K is the radius of the LFR) to map the disk (LFR) to the block.

5) Transform the $2R_K \times 2R_K$ image using the Contourlet transform, search the low frequency regions of the directional sub-band to be embedded, and calculate the pseudo-Zernike moment for these regions. The watermark signal is generated by using the quantification of the modulation of the pseudo-Zernike torque amplitude. The quantitative rule is defined as follows:

$$A'_{p_i q_i} = \left[\frac{A_{p_i q_i} - d(w_i)}{\Delta} \right] \Delta + d(w_i) \quad (i = 1, \ldots L) \tag{9}$$

6) Generate watermarked images. First, the pseudo-Zernike moment for the LFR image $f^*(x, y)$ reconstruction is modified by:

$$f^*(x, y) = f_O(x, y) - f_Z(x, y) \tag{10}$$

where $f_O(x, y)$ is the original LFR image and $f_Z(x, y)$ denotes the modified reconstruction image of the pseudo-Zernike moment:

$$f_Z(x, y) = \sum_{i=1}^{L} Z_{p_i q_i} V_{p_i q_i}(\cdot) + Z_{p_i, -q_i} V_{p_{i,,} - q_i}(\cdot) \tag{11}$$

Second, the pseudo-Zernike moment for the image $f_{Z'}(x, y)$ reconstruction is modified by:

$$f_{Z'}(x, y) = \sum_{i=1}^{L} Z'_{p_i q_i} V_{p_i q_i}(\cdot) + Z'_{p_i, -q_i} V_{p_{i,,} - q_i}(\cdot) \tag{12}$$

7) Reconstruct the CT to obtain the watermarked image. The zero-removal operation is used on each watermarked block to obtain the watermarked disk ok*. After that, ok* is substituted for ok. Repeat steps (4)–(7), until all LFRs are used. Then the watermarked image is obtained.

5 Watermark Detection Algorithm

Generally, watermark detection is the inverse process of watermark embedding. In this paper, the detection process can be divided into five steps:

1) The original watermark $W = \{w_i, i = 1, \cdots, L\}$ is extracted according to the key K_1.

2) The Harris-Laplace detector (see Section 2) is used to process the host image. We can extract many feature points ($\widetilde{P} = \left\{ \widetilde{p}_i \ , i = 1, \cdots, n \right\}$) regarded as the reference centers of the local feature regions.

3) Our proposed method is used to construct a set of local feature regions $\widetilde{O} = \{ \widetilde{o}_k \ , k = 1, \cdots, m \}$.

4) The zero-padding operation is performed on each $\widetilde{o}_k \in \widetilde{O}$ and the normalization procedure is used to process each block of size $2R_K \times 2R_K$ to map the disk (LFR) to the block of size $2R_K \times 2R_K$ (where R_K is the radius of the LFR).

5) The Contourlet is used to transform the $2R_K \times 2R_K$ image by extracting the low frequency area of the directional sub-band in the low frequency regions calculated using the pseudo-Zernike moment. The embedding process uses the following expression.

$$(A^{'}_{p_i q_i})_{Q_j} = \left[\frac{A^{'}_{p_i q_i} - d(j)}{\Delta} \right] \Delta + d(j) \quad (j = 0,1) \tag{13}$$

Through the above expression, we can obtain the two sets of vectors $(A^{'}_{p_i q_i})_0$ and $(A^{'}_{p_i q_i})_1$, $i = 1,..., L$.

The following definition of wi' gives the result of the detection:

$$w_i^{'} = \arg\min_{j \in \{0,1\}} \left((A^{'}_{p_i q_i})_{Q_j} - (A^{'}_{p_i q_i}) \right)^2 (i = 1, \ldots, L) \tag{14}$$

If wi′=0 then the watermarking detection fails; otherwise, if wi′=1 then the watermarking detection is successful. When at least two disks are determined to be watermarked, the final detection is labeled as a success; otherwise, it fails.

6 Simulation Results

We conduct experiments to verify the effectiveness of our proposed method and compare it with the method in [17]. The proposed watermarking scheme is tested on the standard 512 × 512 pixel test images Lena, Baboon, and Pepper. The watermark pattern is a 16-bit pseudo random binary sequence. The watermark is embedded in the perceptually textured region and is therefore less visible.The comparison of the detection results under common signal processing and de-synchronization attacks are shown in Table 1 and Table 2. Each result is expressed as the ratio between the number of correctly detected watermarked LCRs and the number of original embedded watermarked LCRs.

Table 1. The watermark detection results for common signal processing attacks (detection rates)

Attacks	Lena		Baboon		Pepper	
	Proposed scheme	Scheme in [17]	Proposed scheme	Scheme in [17]	Proposed scheme	Scheme in [17]
Median filter(3×3)	6/9	3/10	10/12	3/9	8/11	1/12
Sharpening (3×3)	4/9	8/10	8/12	4/9	7/11	4/12
Salt&Pepper noi (0.02)	5/9	2/10	7/12	5/9	5/11	2/12
Gaussian noise(3×3)	5/9	4/10	9/12	4/9	6/11	1/12
Sharpening(3×3)+JPEG70	4/9	2/10	7/12	4/9	4/11	3/12
Median filter(3×3) +JPEG70	3/9	2/10	6/12	2/9	3/11	2/12

Table 2. The watermark detection results for de-synchronization signal processing attacks

Attacks		Lena		Baboon		Pepper	
		Proposed scheme	Scheme in [17]	Proposed scheme	Scheme in [17]	Proposed scheme	Scheme in [17]
Removed 1 row and 3 columns		7/9	5/10	9/12	6/9	5/8	5/12
Removed 5 rows and 10 columns		6/9	4/10	7/12	3/9	3/8	4/12
Centered cropping 5% off		5/9	3/10	6/12	3/9	4/8	3/12
Centered cropping 10% off		5/9	4/10	5/12	2/9	3/8	2/12
-x-shearing5%, -y-shearing 5%		4/9	2/10	4/12	2/9	3/8	2/12
Shearing 60%		3/9	1/10	3/12	3/9	3/8	2/12
Rotation 5		4/9	2/10	4/12	2/9	3/8	2/12
Rotation 10		3/9	1/10	3/12	2/9	2/8	1/12
Translation-x-10 and –y-10		7/9	4/10	6/12	4/9	5/8	4/12
Scaling	0.8	5/9	1/10	4/12	2/9	4/8	4/12
	1.4	3/9	2/10	5/12	3/9	3/8	3/12
Local random bending		4/9	3/10	6/12	4/9	3/8	2/12
Removed 5 rows and10 columns and Scaling 0.8		3/9	2/10	4/12	3/9	3/8	1/12
Removed 5 rows and10 columns and +JPEG70		4/9	3/10	5/12	3/9	5/8	1/12
Centered cropping 5%+ Rotation 10		4/9	2/10	4/12	2/9	3/8	2/12

7 Conclusion

In this paper, we propose a robust image watermarking scheme based on scale-space theory to resist common signal-processing and even de-synchronization attacks. The key characteristics of the proposed scheme are:

1) The CT provides multiresolution analysis and directional preservation, which provides robustness against translation and noise attacks.
2) Under various attacks, the feature points extracted by the Harris-Laplace detector are reliable, which facilitates re-synchronization between watermark embedding and detection.

In addition, our proposed method can extract the watermark without using the original image and has a low computational complexity rendering it applicable to many different situations.

References

1. Dragoi, I.C., Coltuc, D.: Local prediction based difference expansion reversible watermarking. IEEE Trans. Image Process. **23**, 1779–1790 (2014)
2. Bad, P., Furon, T.: A new measure of watermarking security: the effective key length. IEEE Trans. on Infor. Forensics and Security **43**, 1306–1317 (2013)
3. Harish, N.J., Kumar, B.B.S., Kusagur, A.: Hybrid robust watermarking techniques based on DWT, DCT, and SVD. Int. J. Adv. Electron. Eng. **2**(5), 137–143 (2013)
4. Singh, S.P., Rawat, P.: A robust watermarking appoach using DCT-DWT. Int. J. Emerg. Technol. Adv. Eng., 300–305 (2012)
5. Awasthi, M., Lodhi, H.: Robust image watermarking based on discrete wavelet transform, discrete cosine tranform & singular value decomposition. Adv. Electron. Eng., 971–976 (2014)
6. Jayalakshmi, M., Merchant, S.N., Desai, U.B.: Significant pixel watermarking using human visual system model in wavelet domain. In: Kalra, P.K., Peleg, S. (eds.) ICVGIP 2006. LNCS, vol. 4338, pp. 206–215. Springer, Heidelberg (2006)
7. Jiao, L.C., Tan, S., Liu, F.: Ridgelet theory: From ridgelet transform to curvelet. Chinese J. Engrg. Math. **22**, 761–773 (2005)
8. Starck, J.L., Candes, E., Donoho, D.: The Curvelet Transformfor Image Denoising. IEEE Trans. Image Processing **11**, 670–684 (2002)
9. Do, M.N., Vetterli, M.: The Contourlet transform: an efficient directional multiresolution image representation. IEEE Transactions on Image Processing **14**(12), 2091–2106 (2005)
10. da Cunha, L., Zhou, J., Do, M.N.: The Nonsubsampled Contourlet Transform: Theory, Design, and Applications, 3089–3101 (2004)
11. Cunha, A.L., Zhou, J., Do, M.N.: Nonsubsampled contourilet transform: filter design and applications in denoising. In: IEEE International Conference on Image Processing, vol. 1, pp. 749–752 (2005)
12. Zheng, D., Zhao, J., Saddik, A.E.: RST-invariant digital image watermarking based on log-polar mapping and phase correlation. IEEE Trans. Circuits Syst. Vid. Tech. **13**, 753–765 (2003)
13. Zheng, D., Liu, Y., Zhao, J., Saddik, A.E.: A survey of RST invariant image watermarking algorithms. ACM Comput. Surv. **39**(2), 1–91 (2007)

14. Hao, Y., Bao, G., Zhang, H.: Secure public digital watermarking detection scheme. In: Congress on Image and Signal Processing, CISP 2008, vol. 5, pp. 725–729 (2008)
15. Bas, P., Chassery, J.M., Macp, B.: Geometrically invariant image watermarking based on statistical features in the low-frequency domain. IEEE Tranc. Circ. Sys. Video Technol. **18**(6), 777–90 (2008)
16. Chen, J., Yao, H., Gao, W., Liu, S.: A robust watermarking method based on wavelet and Zernike transform. In: Proceedings of the 2004 International Symposium on Circuits and Systems, ISCAS 2004, vol. 2, pp. 173–176 (2004)
17. Yuan, X.C., Pun, C.M.: Geometrically invariant image watermarking based on feature extraction and Zernike transform. Int. J. Secur. Appl. **6**(2), 217–222 (2012)